Neomangiferin, a Naturally Occurring Mangiferin Congener, Inhibits Sodium-Glucose Co-transporter-2: An *In silico* Approach

Bioinformatics and Biology Insights
Volume 18: 1–9

DOI: 10.1177/11779322231223851

Ayobami J Olusola[1], Samson O Famuyiwa[2], Kolade O Faloye[2], Oluwaseun E Olatunji[3], Uduak I Olayemi[4], Abiodun A Adeyemi[2], John O Balogun[5], Seun B Ogundele[6], Blessing O Babamuyiwa[4] and Rajesh B Patil[7]

[1]Department of Pharmacology, Faculty of Pharmacy, Federal University of Oye Ekiti, Oye-Ekiti, Nigeria. [2]Department of Chemistry, Faculty of Science, Obafemi Awolowo University, Ile-Ife, Nigeria. [3]Department of Pharmaceutical Chemistry, Faculty of Pharmacy, Obafemi Awolowo University, Ile-Ife, Nigeria. [4]Department of Pharmacognosy, Faculty of Pharmacy, Obafemi Awolowo University, Ile-Ife, Nigeria. [5]Department of Chemistry, School of Science, Kogi State College of Education (Technical) Kabba, Kabba, Nigeria. [6]Department of Pharmacognosy and Natural Products, College of Pharmacy, Afe Babalola University, Ado-Ekiti, Nigeria. [7]Department of Pharmaceutical Chemistry, Sinhgad Technical Education Society's, Sinhgad College of Pharmacy, Vadgaon (Bk), Pune, India.

ABSTRACT: Type 2 diabetes is a major health concern contributing to most of diabetic cases worldwide. Mangiferin and its congeners are known for their diverse pharmacological properties. This study sought to investigate the inhibitory property of naturally occurring mangiferin congeners on sodium-glucose co-transporter 2 protein (SGLT-2) using comprehensive computational methods. The naturally occurring mangiferin congeners were subjected to molecular docking, molecular dynamics (MDs) simulation (100 ns), molecular mechanics Poisson-Boltzmann surface area (MM-PBSA) binding free energy, density functional theory calculations (B3LYP 6-31G basis set), and ADMET approaches to identify potential SGLT-2 inhibitor. The molecular docking studies revealed neomangiferin (−9.0 kcal/mol) as the hit molecule compared with dapagliflozin (−8.3 kcal/mol). Root-mean-square deviation (RMSD) and root-mean-square fluctuation (RMSF) plots from the MD simulations established that neomangiferin stabilizes SGLT-2 better than the dapagliflozin, a standard drug. The MM-PBSA binding free energy calculations showed that neomangiferin (−26.05 kcal/mol) elicited better binding affinity than dapagliflozin (−17.42 kcal/mol). The electronic studies showed that neomangiferin (3.48 eV) elicited high electrophilicity index compared with mangiferin (3.31 eV) and dapagliflozin (2.11 eV). Also, the ADMET properties showed that the hit molecule is safe when administered to diabetic subjects. The current *in silico* studies suggest that neomangiferin could emerge as a promising lead molecule as a SGLT-2 inhibitor.

KEYWORDS: Mangiferin congeners, sodium-glucose co-transporter 2 protein, molecular docking, molecular dynamics simulation, density functional theory

RECEIVED: June 14, 2023. **ACCEPTED:** December 14, 2023.

TYPE: Original Research Article

FUNDING: The author(s) received no financial support for the research, authorship, and/or publication of this article.

DECLARATION OF CONFLICTING INTERESTS: The author(s) declared no potential conflicts of interest with respect to the research, authorship, and/or publication of this article.

CORRESPONDING AUTHOR: Kolade O Faloye, Department of Chemistry, Faculty of Science, Obafemi Awolowo University, Ile-Ife 23401, Nigeria. Email: kollintonx1@gmail.com

Introduction

Type 2 diabetes, diabetes mellitus, is a major health burden that affects more than 90% of the world population currently living with the noncommunicable disease, and its prevalence continues to increase yearly.[1] The existing synthetic glucose lowering agents are presented with side effects and various known complications that adversely affect the quality of life of diabetic patients.[2] Therefore, the search for new therapeutic agent, most importantly, those that could effectively inhibit or activate the enzymes associated with the disease, is the need of ongoing efforts in reducing the health burden of diabetes mellitus.

Glucose reabsorption occurs in the kidney which prevents its appearance in the urine.[3] The combination of enzymes such as SGLT-2, glucose transporter 2 (GLUT2), sodium-glucose co-transporter protein 1 (SGLT1), and glucose transporter 1 (GLUT1) is implicated in the uptake of glucose from the urine and subsequent transport of glucose to the blood stream.[4] The inhibition of the SGLT1 resident in the L cell of the proximal small intestine increases plasma glucagon-like peptide 1 (GLP-1) release, reduced postprandial hyperglycaemia, and renoprotective effects.[5-8] The synergistic action of SGLT1 and GLUT2 is responsible for effective glucose absorption in the intestine.[9] Under functional physiological condition, the SGLT-2 is responsible for the uptake of about 90% glucose reabsorption.[10] In addition, an overexpression of the SGLT-2 transporter is observed under hyperglycaemic condition leading to increased glucose reabsorption, which results in increased blood glucose level in diabetic patients.[11] Hence, the inhibition of SGLT-2 to

prevent the renal glucose reabsorption, renal functional impairment, and heart failure in type 2 diabetes patient could be an important mechanism to manage diabetes mellitus.[12,13]

Various synthetic SGLT-2 inhibitors such as dapagliflozin, empagliflozin, and canagliflozin have been introduced as therapeutic agent to manage diabetes.[14] However, the usage of these drugs is presented with episodes of side effects such as kidney damage and urinary tract infections.[14,15] Therefore, there is need to explore natural products as possible and suitable SGLT-2 inhibitor with little or no side effect. Mangiferin congeners are chemical compounds that have an aglycone mainly xanthone and attached to one or more carbohydrate unit through a carbon-carbon linkage.[16] They possess varieties of biological activities such as antioxidant, anti-inflammatory, antimicrobial, antifungal, and anticancer activities.[17-19] Mangiferin and its congeners have become desirable antidiabetic agents due to their resistance to enzymatic and acidic cleavage of the C-C glycosidic bond of their chemical structure.[20] Hence, they may be suitable as potential SGLT-2 inhibitor.

Molecular docking and MD simulation are computational techniques used to screen chemical compounds and study their stability, binding mode, and interactions against the target enzymes implicated in the pathophysiology of metabolic and parasitic diseases.[21,22] The screening technique has become useful due to the fact that it is cheap, fast, and effective in identifying drug candidates.[23] Furthermore, the density functional theory is a computational method that is used to provide useful information about the quantum chemical properties and often predict the druggability of chemical compounds.[24] Though mangiferin is a widely explored pharmacologically, its congeners which have similar structural similarities with different substituents are yet have not been investigated for their SGLT-2 inhibitory property.

Hence, this study uses molecular docking and MD simulation to identify potential SGLT-2 inhibitor among the naturally occurring mangiferin congeners. It also uses density functional theory to evaluate and compare the quantum chemical property of the hit molecule with dapagliflozin (standard drug).

Materials and Methods

Protein and ligand preparation

The three-dimensional (3D) X-ray crystallographic structure of SGLT-2 enzyme (PDBID: 3DH4) was downloaded from the protein data bank (www.rcsb.org). The protein was loaded on PyMol software and water molecules; co-factor and ions were removed to obtain a bare protein suitable for docking. Since the protein does not have a native ligand, the CASTp server was used to identify the amino acid residues resident at the active site for docking purpose (supplemental material, Table S1).

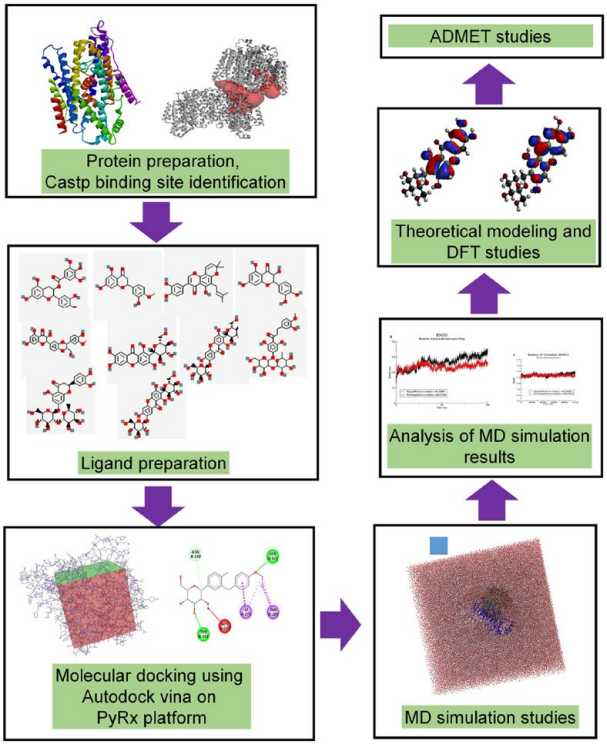

Figure 1. Graphical abstract of the entire *in silico* studies reporting the mangiferin congeners as SGLT1 inhibitors.
SGLT1 indicates sodium-glucose co-transporter protein 1.

Ten naturally occurring mangiferin congeners previously isolated from medicinal plants (supplemental material, Table S2)[25-28] were downloaded from the PubChem database in SDF format, while those that were not available on the database were built with Spartan 14 programme.[29] The ligands were loaded on the built-in open label functionality of PyRx 0.8 software[30] for energy minimization under the MMFF94x force field. The energy-minimized ligands were saved in PDB format for docking purpose. The entire process of *in silico* studies is illustrated in Figure 1.

Molecular docking

The bare SGLT-2 protein and ligands were loaded into the built-in Autodock Vina[31] feature of PyRx 0.8 software and subsequently converted to PDBQT format[32,33] The residues identified at the active site of the protein were selected, and the grid box size was set at centre ($x = 25.5054$, $y = -32.4950$, and $z = 62.3184$) and size ($x = 45.5073$, $y = 46.2700$, and $z = 50.9413$). Then, the ligands were docked into the protein's binding pocket on Autodock Vina at an exhaustiveness of 100.[33] The results obtained were ranked based on their binding energy, and the ligand with the best binding energy was selected at the lowest RMSD value and the best conformation. Thereafter, the protein-ligand interactions such as hydrogen bond, hydrophobic and pi-interactions were examined using the Discovery Studio Visualizer software.[34,35]

Table 1. Interactions of hit molecules with the amino acid residues at receptor sites of SGLT-2.

LIGAND (PUBCHEM ID)	BINDING ENERGY (KCAL/MOL)	HYDROGEN BOND INTERACTION		HYDROPHOBIC INTERACTION	PI-INTERACTION
		AMINO ACID RESIDUE	DISTANCE (Å)		
Neomangiferin (CID 6918448)	−9.0	Glu68,Tyr138, Asn142, Ser372	2.22, 1.98, 2.44, 2.78, 2.61	Ile270, Met369	Ile270, Met369
Dapagliflozin (CID 9887712)	−8.3	Tyr262, Ser372	2.09, 2.26	Ile270, Met369	Tyr269, Ile270, Ser372

Abbreviation: SGLT-2, sodium-glucose co-transporter 2 protein.

Molecular dynamics simulation

The MD simulation of protein-ligand complexes was performed using GROMACS 2023[36],[37] software which was installed in Ubuntu 18.04 LTS on a GPU-enabled PC having the NVIDIA Geforce RTX 3070 graphics card. Docked structures of the protein-ligand complexes were used as starting points in the simulation study. Proteins were processed and the topology files prepared by using pdb2gmx and charmm36 force field[38] while the ligand topology files were prepared by using the online server, SwissParam.[39] The solvent (using the TIP3P water model)[40] addition was done in a cubic box by using a box distance 1.0 nm from the closest atom in the protein. There was no need to add ions to the system since the overall charge was zero. Energy minimization was done by using the steepest descent algorithm taking 50 000 steps and 5 kJ/mol maximum forces. Position restraints were applied in the equilibration step. After that, NVT equilibration was done at 300 K for 100 ps and NPT equilibration taking Parrinello-Rahman (pressure coupling), 1 bar reference pressure for 100 ps. LINCS algorithm was applied to constraint all the bonds. For long-range electrostatics, particle-mesh Ewald (PME) algorithm[41] was used. Finally, the production MD of the protein-ligand complex was run for 100 ns. After successful completion of MD simulation for 100 ns, RMSD of backbone residues, RMSF, radius of gyration (Rg), and solvent accessible surface area (SASA) were calculated. The clustering of the trajectory was done using the gmx_cluster module of the GROMACS programme with an RMSD cut-off of 0.2 nm.

The free energy of binding calculations was done using the stand-alone programme, gmx_MMPBSA by Valdes-Tresanco,[42] based on the MMPBSA.py (from AMBER) functionalities, a well-known and excellent tool for performing end-point binding free energy calculations and to predict the stability of the complex. In this study, MM-PBSA method was employed to calculate the binding free energy between the SGLT-2 protein and the ligands.

Theoretical modelling and optimization studies

DFT studies of neomangiferin, mangiferin, and dapagliflozin were performed using the Spartan 14 software containing functional B3LYP (Lee-Yang Parr exchange-correlation functional method). Also, a 6-31G basis set was selected for the DFT study.[43] During the calculations, the values of the frontier orbital energies for neomangiferin, mangiferin, and dapagliflozin were estimated from the most established conformation of the compounds. In addition, global reactive descriptors such as energy gap (ΔE_{gap}), chemical potential (μ), chemical hardness (η), electronegativity (χ), softness (S), and electrophilicity index were calculated using the formulas below.

$$\Delta E = E_{\mathrm{LUMO}} - E_{\mathrm{HOMO}} \quad (1)$$

$$\eta = -\left(E_{\mathrm{LUMO}} - E_{\mathrm{HOMO}}\right) \quad (2)$$

$$\mu = -\left(E_{\mathrm{LUMO}} + E_{\mathrm{HOMO}}\right) \quad (3)$$

$$\omega = \frac{\mu}{\eta} \quad (4)$$

$$\mathrm{S} = \frac{}{\eta} \quad (5)$$

ADMET studies

ADMET is an acceptable method of investigating the pharmacokinetic properties of potential bioactive phytochemicals that could be effective in the treatment of diseases. In this study, the admetSAR 2.0 server (http://lmmd.ecust.edu.cn/admetsar2/) was used to probe the pharmacokinetic properties of neomangiferin. The ADMET parameters considered include solubility, blood-brain barrier (BBB), nephrotoxicity, hepatotoxicity, carcinogenicity, and oral acute toxicity.

Results and Discussion

Results and discussion

Molecular docking study was performed on mangiferin congeners to estimate their binding energy and possible interaction with the amino acid residues at the active site of SGLT-2 protein. The binding energies observed were compared with dapagliflozin (standard drug) which was set as the cut-off point, and its interaction is presented in Table 1.

Neomangiferin elicited a binding energy of −9.0 kcal/mol showing that it had better binding energy as compared with

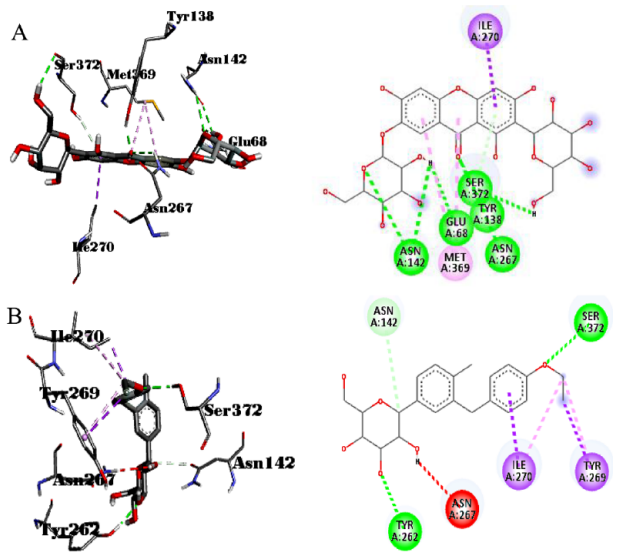

Figure 2. Diagrammatic representation of interaction of (A) neomangiferin-3DH4 and (B) dapgliflozin-3DH4.

dapagliflozin (−8.3 kcal/mol) and mangiferin (−8.5 kcal/mol) which could be obtained from the cleavage of the O-glucose attachment to the neomangiferin moiety. Neomangiferin established 6 hydrogen bonding interactions with the amino acid residues resident at the binding pocket of SGLT-2 enzyme (Glu68H at 2.22 Å, Tyr138-O at 1.98 Å, Asn142-O at 2.44 Å, Asn142H at 2.78 Å, and Ser372H at 2.61 Å), while dapagliflozin formed 2 hydrogen bonding interactions with Tyr262-O at 2.09 Å and Ser372-O at 2.26 Å (Figure 2A and B). Neomangiferin was also stabilized at the binding pocket of SGLT-2 enzyme through the formation of hydrophobic and pi-interactions (pi-alkyl and pi-sigma) with Ile270 and Met369. The formation of higher hydrogen bonding, hydrophobic and pi-interactions was noticed in the protein-ligand complex of neomangiferin. The high number of hydrogen bond formed by neomangiferin showed that the binding pocket of the receptor is less hydrophobic. Hydrophobic interaction has direct influence on the binding energy of a ligand.[44] The lipophilic atoms of neomangiferin established good hydrophobic interaction with the nonpolar side chains of binding site residues of SGLT-2, thereby increasing its binding energy as compared with dapagliflozin.

Neomangiferin has xanthone moiety as its aglycone and 2 glucose attachment at C-C and O-C linkage. The O-C linkage differentiates it from mangiferin which has been identified with promising biological properties. In this study, the attachment of O-C linkage of glucose from neomangiferin improved its binding energy compared with mangiferin, thereby identifying the former as a better SGLT-2 inhibitor compared with dapagliflozin and mangiferin. Previous studies have elucidated the mechanism of action by which neomangiferin ameliorate nonalcoholic fatty liver disease whereby diabetes markers and lipid profiles were effectively managed.[45,46] Neomangiferin was isolated from *Anemarrhena asphodeloide* and *Rhizoma Anemarrhenae* which demonstrated excellent antidiabetic activity.[47,48] It may be inferred that the phytochemical may be among the therapeutic agents responsible for its activity.

Analysis of molecular dynamic simulation

Neomangiferin and dapagliflozin (standard drug) were selected for 100 ns MD simulation to understand their binding mode and dynamic behaviour in the binding pocket of SGLT-2 enzyme.

Root-mean-square deviation

The RMSD plot was obtained to examine the structural stability of neomangiferin and dapagliflozin with the SGLT-2 protein (Figure 3A). In the RMSD trajectories of the ligand-bound system, the graph line of neomangiferin-3DH4 complex showed an increasing trend of RMSD values ranging from 0.2 to 0.29 nm between 0 and 25 ns, indicating that neomangiferin accustomed itself earlier in the binding pocket of the enzyme. A slight deviation was observed between 26 and 45 ns but was within 0.2 to 0.26 nm, after which a stable system was observed from 46 to 100 ns. Dapagliflozin-3DH4 RMSD plot showed deviation from 0 to 30 ns with an increasing trend of RMSD values ranging from 0.2 to 0.3 nm. A stable system was observed between 31 and 65 ns followed by consistent deviation from 66 to 100 ns. The RMSD plots of neomangiferin-3DH4 and dapagliflozin-3DH4 complexes suggested that neomangiferin adapted to conformational changes as the simulation progressed and achieved stability than dapagliflozin.

Root-mean-square fluctuation

The RMSF plots of the neomangiferin-3DH4 and dapagliflozin-3DH4 complexes were examined to estimate their extent of flexibility during the 100 ns simulation period. These estimated fluctuations helped to determine the mobility of the backbone atoms in the neomangiferin-3DH4 and dapagliflozin-3DH4 simulation. Figure 3B shows the RMSF plot of the protein-ligand complexes, indicating that the amino acid residues of the ligand-bound complexes are relatively stable. Also, the RMSF values of neomangiferin-3DH4 ranged from 0.02 to 0.44 nm and dapagliflozin-3DH4 from 0.02 to 0.26 nm.

Radius of gyration

The study assessed the influence of the ligand binding mode on the overall compactness of the protein. Hence, the Rg was estimated, in that, ligand that has higher Rg value elicited higher flexibility, which results instability of the system. Also, a lower Rg value corresponds to a closely packed and dense system and increased stability.[49] The Rg value of neomangiferin-3DH4 and dapagliflozin-3DH4 complexes ranged between 2.3 and 2.33 nm, indicating that there was no significant change in the parking of ligand to the SGLT-2 enzyme (Figure 3C). Also, the Rg of the complexes reached a stable equilibrium throughout the entire 100 ns simulation period.

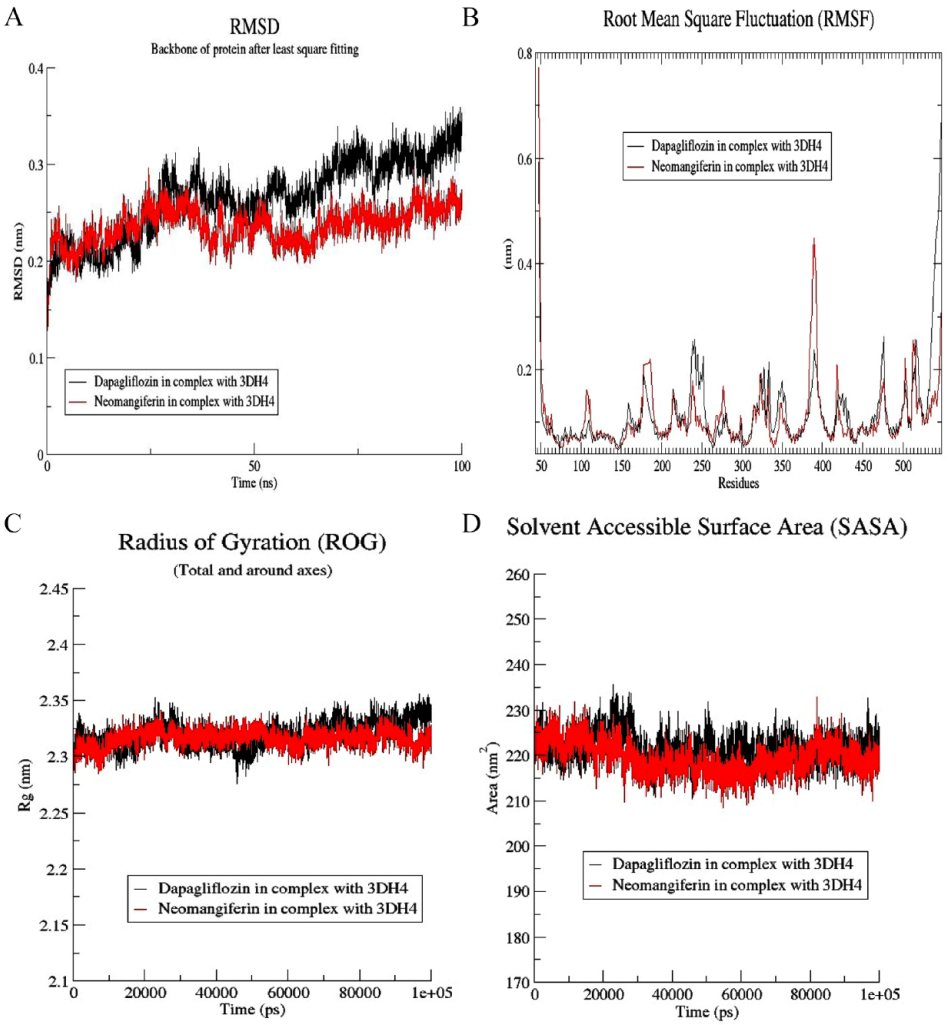

Figure 3. Molecular dynamic simulation plots: (A) RMSD; (B) RMSF; (C) Rg; and (D) SASA.
RMSD indicates root-mean-square deviation; RMSF, root-mean-square fluctuation; Rg, radius of gyration; SASA, solvent accessible surface area.

Solvent accessible surface area

The SASA helps to investigate the surface area of the protein in contact with the solvent in the simulation system.[50] The connectivity between the protein-ligand complexes and the water molecules is estimated from SASA. The change in SASA for neomangiferin-3DH4 and dapagliflozin-3DH4 complexes was analysed during the 100 ns simulation period (Figure 3D). The SASA for neomangiferin-3DH4 and dapagliflozin-3DH4 complexes was 210 to 230 nm^2 and 215 to 235 nm^2, respectively. The data obtained from the analysis showed that there was no large difference in the SASA values when the ligands bind to the protein. In both the systems SASA decreased and stabilized after around 25 ns indicating adaptation of respective ligands in the binding site.

Molecular mechanics Poisson–Boltzmann surface area analysis

The MM-PBSA method was adopted to evaluate the binding affinity of the simulated complexes. In this study, the snapshots of the entire trajectories obtained during the 100 ns simulation were input to estimate the vital forces between the ligand and protein interactions. The total binding free energies calculated for neomangiferin and dapagliflozin are presented in Table 2.

The average binding free energy of the neomangiferin-3DH4 and dapagliflozin-3DH4 is -26.05 ± 0.11 and -17.42 ± 0.12 kcal/mol. Neomangiferin elicited the good binding energy compared with dapagliflozin due to lower electrostatic energy and G_{Gas} value obtained in the free binding energy calculations. This indicates that neomangiferin exhibited favourable binding strength than dapagliflozin.

Frontier molecular orbital and chemical reactivity descriptors

Frontier molecular orbital (FMO) theory explains mechanisms of reaction of organic molecules and provides a clear understanding of the interaction of drug molecules and their receptors.[51,52] Researchers have adopted FMO theory to investigate structure-activity relationships of small structural drugs.

Table 2. Molecular mechanics Poisson-Boltzmann surface area analysis of the protein-ligand complexes.

COMPOUNDS	VAN DER WAAL ENERGY (KCAL/MOL)	ELECTROSTATIC ENERGY (KCAL/MOL)	POLAR SOLVATION ENERGY (KCAL/MOL)	NONPOLAR SOLVATION ENERGY (KCAL/MOL)	TOTAL GAS-PHASE ENERGY (KCAL/MOL)	TOTAL SOLVATION ENERGY (KCAL/MOL)	TOTAL (KCAL/MOL)
Neomangiferin	−47.09 ± 0.09	−53.55 ± 0.22	80.07 ± 0.25	−5.48 ± 0.02	−100.6 ± 40.27	74.59 ± 0.25	−26.05 ± 0.11
Dapagliflozin	−48.03 ± 0.05	−18.56 ± 0.11	54.07 ± 0.13	−4.9 ± 0.00	−66.6 ± 0.12	49.17 ± 0.13	−17.42 ± 0.12

Abbreviation: MM-PBSA, molecular mechanics Poisson-Boltzmann surface area.

Table 3. Quantum chemical properties of neomangiferin, mangiferin, and dapagliflozin.

PARAMETERS	NEOMANGIFERIN	MANGIFERIN	DAPAGLIFLOZIN
E_{LUMO}	−6.03	−5.78	−5.95
E_{HOMO}	−1.72	−1.63	−0.7
ΔE_{gap}	4.31	4.15	5.25
η	2.16	2.08	2.63
M	−3.89	−3.71	−3.33
ω	3.48	3.31	2.11
Δ	0.47	0.48	0.38
X	3.88	3.71	3.33

Abbreviations: E_{HOMO}, highest occupied molecular orbital energy; E_{LUMO}, lowest unoccupied molecular orbital energy; S, softness; ΔE_{gap}, energy gap; η, hardness; μ, chemical potential; χ, electronegativity; ω, electrophilicity index.

Frontier molecular orbital involves the estimation of the energy of the highest occupied molecular orbital (E_{HOMO}) and energy of the lowest unoccupied molecular orbital (E_{LUMO}). In this study, the structural feature of the hit mangiferin congener (neomangiferin) showed that it has C-C glucose and C-O glucose linkages. However, the C-O glucose linkage is the only differential substituent when compared with the structure of mangiferin. Hence, we investigated the effect O-glucose linkage of neomangiferin on its kinetic stability, biological potential, and reactivity and compared the values obtained with mangiferin and dapagliflozin (standard drug) (Table 3).

The HOMO provides important information on the electron-donating ability of a phytochemical while its electron-accepting property is known through the LUMO value.[53] A higher HOMO value indicates high electron-donating capacity while a lower LUMO value indicates a higher electron-accepting ability.[54] Mangiferin had the highest HOMO value of −5.78 eV, indicating that it had better electron-donating capacity than dapagliflozin (−5.95 eV) and neomangiferin (−6.03 eV). Also, neomangiferin had the highest LUMO value of −1.72 eV indicating that it exhibits the highest electron-accepting capacity as compared with mangiferin (−1.63 eV) and dapagliflozin (−0.70 eV) (Figure 4).

Chemical reactivity descriptors

Chemical reactivity descriptors are parameters adopted by chemists to predict chemical reactivity, relative stability, and possible bioactivity potential of organic compounds.[55] Energy gap, ΔE_{gap}, explains stability and reactivity of phytochemicals.[56] Molecules with higher ΔE_{gap} value are said to be stable but less reactive. Hence, dapagliflozin (5.25 eV) is the most stable and less reactive as compared with neomangiferin (4.31 eV) and mangiferin (4.15 eV). Global hardness, η, is the degree of rigidity of an electron cloud of a molecule to withstand deformation.[57] It directly relates to energy gap, which further confirms stability of organic molecule. In this study, dapagliflozin (2.63 eV) is the most stable followed by neomangiferin (2.16 eV) and mangiferin (2.08 eV).

On the contrary, global softness (δ) is the reciprocal tendency of molecules to accept electrons.[58] A higher global softness value favours massive electron transfer from the atoms of a molecule and also indicates higher reactivity.[59] The order of increasing global softness of the molecules is mangiferin (0.48 eV) >neomangiferin (0.47 eV) >dapagliflozin (0.38 eV). The electrophilicity index (ω) is a measure of the electron-donating ability of a molecule.[60] It also provides vital information on the tendency of a molecule to bind to a receptor implicated in any disease condition.[28] Neomangiferin (3.48 eV) had the highest electrophilicity value thereby justifying the high binding energy obtained in the molecular docking and MD simulation studies. The electrophilicity index is followed by mangiferin (3.31 eV) and dapagliflozin (2.11 eV).

Chemical potential, μ, is the energy change experienced by a molecule in connection with electron number at a fixed potential.[57] It is the probability of a molecule to exchange

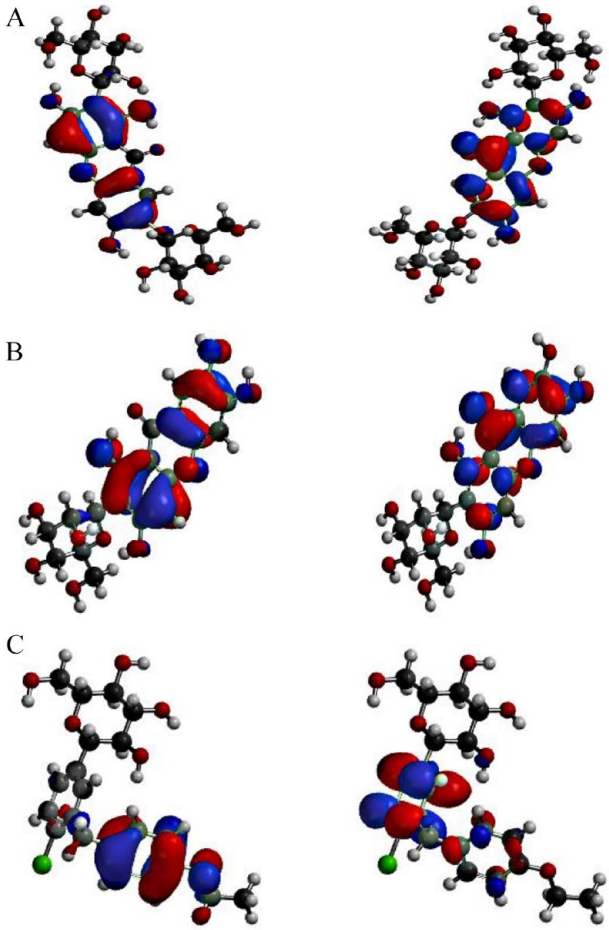

Figure 4. HOMO and LUMO diagrammatic representation of: (A) neomangiferin; (B) mangiferin; and (C) dapagliflozin.
HOMO indicates highest occupied molecular orbital; LUMO, lowest unoccupied molecular orbital.

electron density with the environment at the ground state, and this is connected with ω of molecules. High chemical potential value of molecules (dapagliflozin −3.33 eV and mangiferin −3.71 eV) shows they are weak electrophile and neomangiferin that has lower μ value (−3.89 eV) have strong electrophilic potential. Also, electronegativity (χ) is the characteristic of molecules to attract electrons.[60] A high electronegativity value corresponds to a higher electron withdrawing potential. Neomangiferin (3.88 eV) had the highest electronegativity value, indicating that it has greater electron withdrawing tendency than mangiferin (3.71 eV) and dapagliflozin (3.33 eV). The high electronegativity value of neomangiferin may be as a result of the higher number of oxygen atoms on its chemical structure.

The O-glucose unit of neomangiferin had a higher influence on its electrophilicity value which, in turn, contributed to its binding energy in the docking studies. Also, the increased oxygen atoms contributed by the O-glucose attachment of neomangiferin had direct influence on the E_{LUMO} and electronegativity value of the ligand.

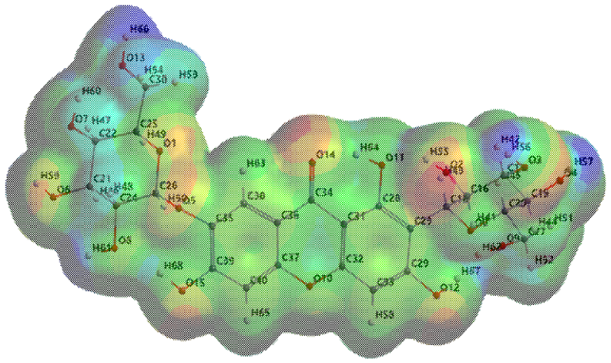

Figure 5. The MEP diagram of neomangiferin.
MEP indicates molecular electrostatic potential.

Molecular electrostatic potential of neomangiferin

The molecular electrostatic potential (MEP) is related to an effective descriptor useful in determining the possible site for nucleophilic and electrophilic attack in a molecule.[60] It is directly related to sites enriched with electron density. Molecular electrostatic potential also gives information about sites that can form hydrogen bonds with other atom.[23] To predict the reactive sites where nucleophilic and electrophilic attack can occur in neomangiferin, the MEP was evaluated using the B3LYP 6-31 (d, p) level geometry of the molecule optimized in the gas phase (Figure 5). In this study, the colours of the electrostatic potential are denoted in blue (nucleophilic region) and red (electrophilic region). Oxygen atoms (O_4, O_9, O_7, O_{12}, O_{14}, and O_{15}) on the xanthone (aglycone) and sugar molecules were the strong electrophilic region, while the electron density was localized on the hydrogen atoms (H_{56}, H_{57}, H_{59}, H_{60}, H_{61}, H_{62}, H_{66}, and H_{67}) to form the nucleophilic region of the neomangiferin moiety. The electron-rich and electron-deficient centres of neomangiferin may be available for hydrogen bonding formation and also strengthen the stability of the phytochemical at the active site of SGLT-2 enzyme.

ADMET properties

The *in silico* approach to probing the ADMET properties of chemical compounds has helped medicinal chemists to identify compounds with potential adverse effect. In this study, the solubility, acute oral toxicity, carcinogenicity, hepatotoxicity, BBB permeability, and nephrotoxicity were examined to understand the pharmacokinetic properties of neomangiferin.

Solubility of a chemical compound explains the extent of its absorption in a diabetic subject.[29] Carcinogenicity and hepatotoxicity properties of phytochemical give relevant information on whether it causes the development of cancerous cells and also maybe it will be toxic to the liver.[61] The nephrotoxicity and acute oral toxicity profile of a ligand helps to understand its safety to the kidney and when taken orally

by diabetic subject.[61] Blood-brain barrier permeability property of a phytochemical explains its ability to cross the BBB layer.[62]

Neomangiferin had a solubility value of −2.196, indicating that it has a good solubility property. A solubility value of −6.0 to 0.5 is preferred for a drug candidate. Also, the acute oral toxicity profile of the phytochemical showed that it is safe when taken orally by a diabetic subject. Furthermore, the nephrotoxicity, hepatotoxicity, and carcinogenicity profile of neomangiferin showed that it is not toxic to the kidney and liver and will not cause the development of cancerous cell. However, neomangiferin could not cross the BBB layer. This property may not be important since the compound is not studied towards the development of a central nervous system drug.[63]

Conclusion

This study used molecular docking, MD simulation, MM-PBSA binding free energy calculations, density functional theory calculations, and ADMET analysis to screen naturally occurring mangiferin congeners as SGLT-2 inhibitor. The computational methods used in the study revealed neomangiferin as a potential SGLT-2 inhibitor and a good drug candidate in the management of type-2 diabetes. The binding energies obtained from the molecular docking studies identified neomangiferin as the top-ranked inhibitor. The RMSD, RMSF, Rg, and SASA plots obtained from the 100 ns MD simulation showed that neomangiferin was more stable in the binding pocket of SGLT-2 enzyme compared with dapagliflozin. Also, neomangiferin elicited better binding energy from the MM-PBSA analysis as compared with dapagliflozin. The influence of the O-glucose attachment was studied using density functional theory calculations. Neomangiferin elicited better electrophilicity index as compared with mangiferin that differs from neomangiferin through the O-glucose substituent. Furthermore, the ADMET studies showed that neomangiferin may exhibit nontoxic properties when administered to diabetic patient. This hit molecule could be useful in the development of SGLT-2 *in vivo* and *in vitro*.

Author Contributions

AJO: Conceptualization, methodology, original draft preparation. SOF: Supervision, review and editing. KOF: Conceptualization, supervision, methodology, data curation, original draft preparation, review and editing. OEO: Methodology, original draft preparation, UIO: Investigation, review and editing. AAA: Investigation, original draft preparation. JOB: Methodology, data curation, review and editing. SBO: Investigation, data curation, review and editing, BOB: Data curation. RBP: Review and editing.

Supplemental Material

Supplemental material for this article is available online.

REFERENCES

1. Sirdah MM, Reading NS. Genetic predisposition in type 2 diabetes: a promising approach toward a personalized management of diabetes. *Clin Genet*. 2020;98:525-547.
2. Khursheed R, Singh SK, Wadhwa S, et al. Treatment strategies against diabetes: success so far and challenges ahead. *Eur J Pharmacol*. 2019;862:172625.
3. Woods TC, Satou R, Miyata K, et al. Canagliflozin prevents intrarenal angiotensinogen augmentation and mitigates kidney injury and hypertension in mouse model of type 2 diabetes mellitus. *Am J Nephrol*. 2019;49:331-342.
4. Pereira-Moreira R, Muscelli E. Effect of insulin on proximal tubules handling of glucose: a systematic review. *J Diabetes Res*. 2020;2020:8492467.
5. Mima A, Qi W, King GL. Implications of treatment that target protective mechanisms against diabetic nephropathy. *Semin Nephrol*. 2012;32:471-478.
6. Mima A. A narrative review of diabetic kidney disease: previous and current evidence-based therapeutic approaches. *Adv Ther*. 2022;39:3488-3500.
7. Mima A, Nomura A, Fujii T. Current findings on the efficacy of incretin-based drugs for diabetic kidney disease: a narrative review. *Biomed Pharmacother*. 2023;165:115032.
8. Mima A, Gotoda H, Lee R, Murakami A, Akai R, Lee S. Effects of incretin-based therapeutic agents including tirzepatide on renal outcomes in patients with type 2 diabetes: a systemic review and meta-analysis. *Metabol Open*. 2023;17:100236.
9. Primec M, Škorjanc D, Langerholc T, Mičetić-Turk D, Gorenjak M. Specific *Lactobacillus* probiotic strains decrease transepithelial glucose transport through GLUT2 downregulation in intestinal epithelial cell models. *Nutr Res*. 2021;86:10-22.
10. Yakovleva T, Sokolov V, Chu L, et al. Comparison of the urinary glucose excretion contributions of SGLT-2 and SGLT1: a quantitative systems pharmacology analysis in healthy individuals and patients with type 2 diabetes treated with SGLT-2 inhibitors. *Diabetes Obes Metab*. 2019;21:2684-2693.
11. Moradi-Marjaneh R, Paseban M, Sahebkar A. Natural products with SGLT-2 inhibitory activity: possibilities of application for the treatment of diabetes. *Phytother Res*. 2019;33:2518-2530.
12. Mima A. Sodium-glucose cotransporter 2 inhibitors in patients with non-diabetic chronic kidney disease. *Adv Ther*. 2021;38:2201-2212.
13. Mima A. Renal protection by sodium-glucose cotransporter 2 inhibitors and its underlying mechanisms in diabetic kidney disease. *J Diabetes Complications*. 2018;32:720-725.
14. Fitchett DA. Safety update on sodium glucose co-transporter 2 inhibitors. *Diabetes Obes Metab*. 2019;21:34-42.
15. Tentolouris A, Vlachakis P, Tzeravini E, Eleftheriadou I, Tentolouris N. SGLT-2 inhibitors: a review of their antidiabetic and cardioprotective effects. *Int J Environ Res Public Health*. 2019;16:2965.
16. Wolfender JL, Urbain A, Hostettmann K. Profiling, isolation, chemical characterisation and distribution of Gentianaceae constituents. In: Rybczyński, J, Davey, M, Mikuła, A, eds. *The Gentianaceae-Volume 2: Biotechnology and Applications*. Springer; 2015:349-381.
17. Benard O, Chi Y. Medicinal properties of mangiferin, structural features, derivative synthesis, pharmacokinetics and biological activities. *Mini Rev Med Chem*. 2015;15:582-594.
18. Khare P, Shanker K. Mangiferin: a review of sources and interventions for biological activities. *Biofactors*. 2016;42:504-514.
19. Vo THT, Nguyen TD, Nguyen QH, Ushakova NA. Extraction of mangiferin from the leaves of the mango tree *Mangifera indica* and evaluation of its biological activity in terms of blockade of α-glucosidase. *Pharm Chem J*. 2017;51:806-810.
20. Grover P, Mehta L, Malhotra A, et al. Exploring the multitarget potential of iridoids: advances and applications. *Curr Top Med Chem*. 2023;23:371-388.
21. Safavi A, Ghodousi ES, Ghavamizadeh M, et al. Computational investigation of novel farnesyltransferase inhibitors using 3D-QSAR pharmacophore modeling, virtual screening, molecular docking and molecular dynamics simulation studies: a new insight into cancer treatment. *J Mol Struct*. 2021;1241:130667.
22. Alzain AA, Ahmed ZAM, Mahadi MA, Elbadwi FA. Identification of novel *Plasmodium falciparum* dihydroorotate dehydrogenase inhibitors for malaria using *in silico* studies. *Sci Afr*. 2022;16:e01214.
23. Muhseen ZT, Hameed AR, Al-Bhadly O, Ahmad S, Li G. Natural products for treatment of Plasmodium falciparum malaria: an integrated computational approach. *Comput Biol Med*. 2021;134:104415.
24. Awotuya IO, Fakola EG, Olusola AJ, et al. Exploring the protein tyrosine phosphatase 1B inhibitory potentials of naturally occurring brazilin-type homoisoflavonoids: a computational approach. *Chem Afr*. 2022;5:1493-1502.
25. Faizi S, Zikr-ur-Rehman S, Naz A, Versiani MA, Dar A, Naqvi S. Bioassay-guided studies on *Bombax ceiba* leaf extract: isolation of shamimoside, a new antioxidant xanthone C-glucoside. *Chem Nat Compd*. 2012;48:774-779.
26. Finnegan RA, Stephani RA, Ganguli G, Ganguly SN, Bhattacharya AK. Occurrence of mangiferin in *Hiptage madablota* geartn. *J Pharm Sci*. 1968;57:1039-1040.

27. Hong YF, Han GY, Guo XM. Isolation and structure determination of xanthone glycosides of *Anemarrhena asphodeloides*. *Yao Xue Xue Bao = Acta Pharm Sin*. 1997;32:473-475.
28. Aritomi M, Kawasaki T. A new xanthone C-glucoside, position isomer of mangiferin, from *Anemarrhena asphodeloides* Bunge. *Chem Pharm Bull*. 1970;18: 2327-2333.
29. Olajubutu OG, Ogunremi BI, Adewole AH, et al. Topical anti-inflammatory activity of *Petiveria alliacea*, chemical profiling and computational investigation of phytoconstituents identified from its active fraction. *Chem Afr*. 2022;5: 557-565.
30. Ogboye RM, Patil RB, Famuyiwa SO, Faloye KO. Novel α-amylase and α-glucosidase inhibitors from selected Nigerian antidiabetic plants: an *in silico* approach. *J Biomol Struct Dyn*. 2022;40:6340-6349.
31. Trott O, Olson AJ. AutoDock Vina: improving the speed and accuracy of docking with a new scoring function, efficient optimization, and multithreading. *J Comput Chem*. 2010;31:455-461.
32. Ahmad S, Singh V, Gautam HK, Raza K. Multisampling-based docking reveals imidazolidinyl urea as a multitargeted inhibitor for lung cancer: an optimisation followed multi-simulation and in-vitro study. *J Biomol Struct Dyn*. Published online May 8, 2023. doi:10.1080/07391102.2023.2209673
33. Ahmad S, Raza K. Identification of 5-nitroindazole as a multitargeted inhibitor for CDK and transferase kinase in lung cancer: a multisampling algorithm-based structural study. *Mol Divers*. Published online April 14, 2023. doi:10.1007/s11030-023
34. Tripathi MK, Ahmad S, Tyagi R, Dahiya V, Yadav MK. Fundamentals of molecular modeling in drug design. In: Rudrapal, M, Egbuna, C, eds. *Computer Aided Drug Design (CADD): From Ligand-Based Methods to Structure-Based Approaches*. Elsevier; 2022:125-155. doi:10.1016/B978-0-323-90608-1.00001-0
35. Ahmad S, Dahiya V, Vibhuti A, Pandey RP, Tripathi MK, Yadav MK. Therapeutic protein-based vaccines. In: Singh, DB, Tripathi, T, eds. *Protein-Based Therapeutics*. Springer Nature; 2023:355-384. doi:10.1007/978-981-19-8249-1_13
36. Famuyiwa SO, Patil RB, Faloye KO, et al. Sappanin-type homoisoflavonoids from *Scilla nervosa* inhibits acetylcholinesterase enzyme: a combined *in silico* and *in vitro* approach. *J Biomol Struct Dyn*. 2023;41:10957-10968.
37. Fadare OA, Omisore NO, Adegbite OB, et al. Structure based design, stability study and synthesis of the dinitrophenylhydrazone derivative of the oxidation product of lanosterol as a potential *P. falciparum* transketolase inhibitor and in-vivo antimalarial study. *In Silico Pharmacol*. 2021;9:38. doi:10.1007/s40203-021
38. Abraham MJ, Murtola T, Schulz R, Páll S, Smith JC, Hess B. GROMACS: high performance molecular simulations through multi-level parallelism from laptops to supercomputers. *Softwarex*. 2015;1-2:19-25. doi:10.1016/j.softx.2015.06.001
39. Singh R, Bhardwaj VK, Sharma J, Kumar D, Purohit R. Identification of potential plant bioactive as SARS-CoV-2 Spike protein and human ACE2 fusion inhibitors. *Comput Biol Med*. 2021;136:104631.
40. Dodda LS, Cabeza de, Vaca I, Tirado-Rives J, Jorgensen WL. LigParGen web server: an automatic OPLS-AA parameter generator for organic ligands. *Nucleic Acids Res*. 2015;45:331-336.
41. Jorgensen WL, Madura JD. Quantum and statistical mechanical studies of liquids. 25. Solvation and conformation of methanol in water. *J Am Chem Soc*. 1983;105:1407-1413.
42. Petersen HG. Accuracy and efficiency of the particle mesh Ewald method. *J Chem Phys*. 1995;103:3668-3679.
43. Valdés-Tresanco MS, Valdés-Tresanco ME, Valiente PA, Moreno E. Gmx_MMPBSA: a new tool to perform end-state free energy calculations with GROMACS. *J Chem Theory Comput*. 2021;17:6281-6291. doi:10.1021/acs.jctc.1c00645
44. Becke AD. A new mixing of HartreeeFock and local density-functional theories. *J Chem Phys*. 1993;98:1372-1377.
45. Dong J, Davis AP. Molecular recognition mediated by hydrogen bonding in aqueous media. *Angew Chem*. 2021;133:8113-8126.
46. Zhou C, Zhou J, Han N, Liu Z, Xiao B, Yin J. Beneficial effects of neomangiferin on high fat diet-induced nonalcoholic fatty liver disease in rats. *Int Immunopharmacol*. 2015;25:218-228.
47. Miura T, Ichiki H, Iwamoto N, et al. Antidiabetic activity of the rhizoma of *Anemarrhena asphodeloides* and active components, mangiferin and its glucoside. *Biol Pharm Bull*. 2001;24:1009-1011.
48. Han J, Yang N, Zhang F, et al. Rhizoma Anemarrhenae extract ameliorates hyperglycemia and insulin resistance via activation of AMP-activated protein kinase in diabetic rodents. *J Ethnopharmacol*. 2017;172:368-376.
49. En-Nahli F, Baammi S, Hajji H, Alaqarbeh M, Lakhlifi T, Bouachrine M. High-throughput virtual screening approach of natural compounds as target inhibitors of plasmepsin-II. *J Biomol Struct Dyn*. 2023;41:10070-10080.
50. Marsh J, Teichmann S. Relative solvent accessible surface area predicts protein conformational changes upon binding. *Structure (London, England: 1993)*. 2011;19:859-867.
51. Ahsan F, Yar M, Gulzar A, Ayub K. Therapeutic potential of C_2N as targeted drug delivery system for fluorouracil and nitrosourea to treat cancer: a theoretical study. *J Nanostruct Chem*. 2023;13:89-102.
52. Bouback TA, Pokhrel S, Albeshri A, et al. Pharmacophore-based virtual screening, quantum mechanics calculations, and molecular dynamics simulation approaches identified potential natural antiviral drug candidates against MERS-CoV S1-NTD. *Molecules*. 2021;26:4961.
53. Mazzone G, Malaj N, Galano A, Russo N, Toscano M. Antioxidant properties of several coumarin-chalcone hybrids from theoretical insights. *RSC Adv*. 2015;5:565-575.
54. Owoseeni OD, Patil RB, Phage PM, et al. Computational assessment of xanthones from African medicinal plants as aldose reductase inhibitors. *Computation*. 2022;10:146.
55. Domingo LR, Ríos-Gutiérrez M, Pérez P. Applications of the conceptual density functional theory indices to organic chemistry reactivity. *Molecules*. 2016;21:748.
56. Miar M, Shiroudi A, Pourshamsian K, Oliaey AR, Hatamjafari F. Theoretical investigations on the HOMO-LUMO gap and global reactivity descriptor studies, natural bond orbital, and nucleus-independent chemical shifts analyses of 3-phenylbenzo [d] thiazole-2 (3 H)-imine and its para-substituted derivatives: solvent and substituent effects. *J Chem Res*. 2021;45:147-158.
57. Nalini H, Thairiyaraja M, Arunagiri C, et al. Crystal growth, structural, nonlinear, optical and theoretical investigations of L-histidinium trichloroacetate single crystals. *Bull Mater Sci*. 2021;44:1-17.
58. Faloye KO, Adesida SA, Oguntimehin SA, et al. LC-MS analysis, computational investigation, and antimalarial studies of *Azadirachta indica* fruit. *Bioinform Biol Insights*. 2023;17:11779322231154966.
59. Ayeni AO, Akinyele OF, Hosten EC, Fakola EG, Olalere JT, Egharevba GM. Watkins synthesis, crystal structure, experimental and theoretical studies of corrosion inhibition of 2-((4-(2-hydroxy-4-methylbenzyl) piperazin-1-yl) methyl)-5-methylphenol – a Mannich base. *J Mol Struct*. 2020;1219:128539.
60. Ahmed MSM, Mekky AE, Sanad SM. Regioselective [3+ 2] cycloaddition synthesis and theoretical calculations of new chromene-pyrazole hybrids: a DFT-based Parr function, Fukui function, local reactivity indexes, and MEP analysis. *J Mol Struct*. 2022;1267:133583.
61. Sharma A, Sharma S, Gupta M, Fatima S, Saini R, Agarwal SM. Pharmacokinetic profiling of anticancer phytocompounds using computational approach. *Phytochem Anal*. 2018;29:559-568.
62. Fatima S, Gupta P, Sharma S, Sharma A, Agarwal SM. ADMET profiling of geographically diverse phytochemical using chemoinformatic tools. *Future Med Chem*. 2020;12:69-87.
63. Kumar R, Sharma A, Tiwari RK. Can we predict blood brain barrier permeability of ligands using computational approaches? *Interdiscip Sci*. 2013;5:95-101.